PROCEEDINGS OF SCIENCE

Parton Branching TMDs with angular ordering condition and their application to Z boson $p_\perp$ spectrum

Aleksandra Lelek*
UAntwerp
E-mail: aleksandra.lelek@uantwerpen.be

We study the effects of angular ordering constraint on transverse momentum dependent (TMD) parton distributions functions (PDFs) obtained within the Parton Branching (PB) method. We compare it with virtuality and pt ordering definitions. We study the effect of ordering choice on predictions for Z boson $p_\perp$ spectrum, especially at low pt and we demonstrate the advantage of the angular ordering. We compare the PB formalism with another existing and commonly used approaches as Kimber-Martin-Ryskin-Watt (KMRW) and Collins-Soper-Sterman (CSS). Especially, we identify the CSS Sudakov coefficients with the terms in the PB Sudakov form factor.

XXVII International Workshop on Deep-Inelastic Scattering and Related Subjects - DIS2019
8-12 April, 2019
Torino, Italy

*Speaker.

PoS(DIS2019)020

1. Motivation

The powerful tool used to obtain QCD predictions for high energy observables is the collinear factorization theorem [1], based on the assumption that partons move collinearly with the hadron they constitute. Although this approach is extremely successful in many different measurements, there are some observables where also the transverse motion of the partons has to be taken into account to achieve satisfactory precision. This can be fulfilled via the transverse momentum dependent (TMD) factorization theorem [2] in the spirit of high energy $k_\perp$- factorization [3] or Collins-Soper-Sterman [4] formalism. The crucial ingredients of the TMD factorization approaches are the TMD parton distribution functions (PDFs), called TMDs. TMDs can be obtained in a wide kinematic range with the recently developed Parton Branching (PB) method [5, 6, 7].

In this paper we discuss the role of the angular ordering condition, which allows to treat properly the soft gluon colour coherence phenomena. We compare the angular ordering implementation in the PB method with the prescriptions given by Marchesini's and Webber's [9], Kimber-Martin-Ryskin-Watt (KMRW) [10] and Collins-Soper-Sterman (CSS) [4]. We demonstrate the importance of angular ordering for obtaining precision description of Z boson $p_\perp$ spectrum.

2. TMD evolution equation

In the PB method the evolution equation for the momentum weighted TMD $\widetilde{A}_a\left(x,k_\perp,\mu^2\right) = xA_a\left(x,k_\perp,\mu^2\right)$, for a parton species and flavour a, carrying the fraction x of the proton's momentum and having the transverse momentum $k_\perp$ [1] at the evolution scale μ, including not only the collinear evolution but also the transverse momentum at each branching, was proposed [5]

$$\widetilde{A}_a\left(x,k_\perp,\mu^2\right) = \Delta_a\left(\mu^2,\mu_0^2\right)\widetilde{A}_a\left(x,k_\perp,\mu_0^2\right) + \sum_b \int \frac{\mathrm{d}^2\mu'_\perp}{\pi\mu'^2}\Theta\left(\mu^2-\mu'^2\right)\Theta\left(\mu'^2-\mu_0^2\right)\times$$
$$\times\ \Delta_a\left(\mu^2,\mu'^2\right)\int_x^{z_M}\mathrm{d}z P_{ab}^R\left(z,\alpha_s(a(z)^2\mu'^2)\right)\widetilde{A}_b\left(\frac{x}{z},k_\perp+a(z)\mu_\perp,\mu'^2\right)\ . \tag{2.1}$$

Here P_{ab}^R is the real-emission part of the splitting function for a parton b splitting into a parton a which propagates towards the hard scattering, $z = x_a/x_b$ is the splitting variable, $|\mu_\perp| \equiv \mu'$ is the scale at which the branching happens, μ_0 is the initial evolution scale. The Sudakov form factor is defined as $\Delta_a(\mu^2,\mu_0^2) \equiv \Delta_a(\mu^2) = \exp\left[-\int_{\mu_0^2}^{\mu^2}\frac{\mathrm{d}\mu'^2}{\mu'^2}\sum_b\int_0^{z_M}\mathrm{d}z z P_{ba}^R\left(z,\alpha_s\left(a(z)^2\mu'^2\right)\right)\right]$. The function $a(z)$ gives the relationship between the scale of the branching and the transverse momentum of the emitted and propagating parton. For virtuality ordering, the scale of the branching is associated with the virtuality of the propagating parton $q_\perp^2 = (1-z)\mu'^2$ $\left(a(z) = \sqrt{1-z}\right)$. In the limit of $z \to 1$ one obtains $p_\perp$-ordering condition where the scale of the branching is assigned to the transverse momentum of the emitted parton $q_\perp^2 = \mu_\perp'^2$ $(a(z) = 1)$. For angular ordering condition the scale of the branching is associated with energy of the parent parton times the angle of the emitted parton with respect to the beam direction $q_\perp^2 = (1-z)^2\mu_\perp'^2$ $(a(z) = 1-z)$. The relation between the scale of the branching and the transverse momentum gives the constraint on the soft gluon resolution scale parameter z_M. It is fixed to a value very close to 1 for $p_\perp$- ordering or it changes with the

[1] For a given 4-vector $k = (k^0,k^1,k^2,k^3) = (E_k,k_\perp,k^3)$, where $k_\perp = (k^1,k^2)$.

branching scale as $z_M = 1 - \left(\frac{q_0}{\mu'}\right)^2$ for virtuality ordering or $z_M = 1 - \frac{q_0}{\mu'}$ for angular ordering where q_0 is the minimum transverse momentum of the emitted parton with which it can be resolved. The PB method allows one to choose the definition of z_M, the scale in α_s and the way the transverse momentum is related to the branching scale individually [2].

In the PB method the transverse momentum of the propagating parton is a sum of the intrinsic transverse momentum and the transverse momentum of all the emitted partons $k_\perp = k_{\perp 0} - \sum_i q_{\perp,i}$. After integrating eq. (2.1) over the transverse momentum $k_\perp$ one obtains collinear PDF $\int \mathrm{d}k_\perp^2 \widetilde{A}_a\left(x, k_\perp, \mu^2\right) = \widetilde{f}_a\left(x, \mu^2\right)$. In the limit of $z_M \to 1$ and with $\alpha_s(\mu'^2)$ the Dokshitzer-Gribov-Lipatov-Altarelli-Parisi (DGLAP) evolution equation [11] is obtained.

3. Highlights

In fig. 1 we show PB TMDs [3] obtained with $p_\perp$-, virtuality and angular ordering to relate $q_\perp$ and μ', with $\alpha_s(\mu'^2)$, for 3 different fixed values of z_M. As discussed in [5], after integration over the transverse momentum, with all these z_M values and ordering definitions the same collinear PDF is obtained. However, this is not the case for TMDs. Only in the case of angular ordering the cancellation of non-resolvable emissions between real and virtual pieces is taken into account properly and z_M independent results are obtained. For $p_\perp$-ordering the distributions are very much dependent on z_M that is why they are not going to be discussed anymore in this paper. Virtuality ordering works much better than $p_\perp$-ordering but worse than angular ordering.

The PB TMDs were used to test the effect of ordering choice on the prediction of the Z boson $p_\perp$ spectrum in DY process and compared to the ATLAS measurement [12] at 8 TeV. The procedure how the results are obtained is described in [6]. In fig. 2 we present results obtained with the PB TMDs [4] and Pythia leading order (LO) matrix element. The results on the left hand side of fig. 2 are obtained with the angular and virtuality ordering conditions to relate $q_\perp$ and μ' with $z_M = 1 - 10^{-5}$ and $\alpha_s(\mu'^2)$. In the next step, the scale of α_s was changed to be the transverse momentum, which is shown in the right of fig. 2. From fig. 2 one can see the difference between virtuality and angular ordering predictions. Only with angular ordering condition one can reproduce the correct shape of the Z boson $p_\perp$ spectrum. Moreover, for angular ordering, the change of the scale in the running coupling to the transverse momentum leads to better data description. Based on this result, fits of TMDs to precision measurements of deep inelastic scattering (DIS) cross sections at HERA were performed using `xFitter` [8] for angular ordering ($q_\perp^2 = (1-z)^2 \mu_\perp'^2$) in two scenarios: with $\alpha_s(\mu'^2)$ and $\alpha_s(q_\perp^2)$ [6]. A very good description of the Z boson $p_\perp$ spectrum was obtained with $\alpha_s(q_\perp^2)$ which is shown in fig. 3 [6].

4. PB and other approaches

In the following we present the first results obtained with the dynamic z_M.

[2] E.g. one can use angular ordering in the relation between $q_\perp$ and μ' but keeping z_M fixed and $\alpha_s(\mu'^2)$ as in $p_\perp$-ordering to study the effect of each piece of the ordering definition.

[3] The next-to-leading order (NLO) splitting functions and α_s and the default QCDNUM parametrization as the starting distribution are used.

[4] The NLO splitting functions and α_s, with the initial parametrization from HERAPDF2.0 are used

Marchesini and Webber After integration of eq. (2.1) with angular ordering condition over the transverse momentum, the following evolution formula for the collinear distribution is obtained

$$\widetilde{f}_a(x,\mu^2) = \widetilde{f}_a(x,\mu_0^2)\Delta_a(\mu^2) + \int_{\mu_0^2}^{\mu^2} \frac{d\mu'^2}{\mu'^2}\frac{\Delta_a(\mu^2)}{\Delta_a(\mu'^2)}\sum_b \int_x^{1-\frac{q_0}{\mu'}} dz P_{ab}^R(\alpha_s((1-z)^2\mu'^2),z)\widetilde{f}_b(\frac{x}{z},\mu'^2) \quad (4.1)$$

which coincides with the evolution formula of Marchesini and Webber [9] [5].

Kimber-Martin-Ryskin-Watt In this paragraph the PB method is compared with the KMRW approach [10]. For this purpose, the PB formula for angular ordering eq. (4.1) is rewritten in terms of integral over the transverse momentum $q_\perp^2$ instead of the branching scale μ'^2 [6]

$$\begin{aligned}\widetilde{f}_a(x,\mu^2) &= \widetilde{f}_a(x,\mu_0^2)\Delta_a(\mu^2,\mu_0^2) \\ &+ \int_{q_0^2}^{(1-x)^2\mu^2} \frac{dq_\perp^2}{q_\perp^2}\int_x^{1-\frac{q_\perp}{\mu}} dz \Delta_a\left(\mu^2,\frac{q_\perp^2}{(1-z)^2}\right)\sum_b P_{ab}^R\left(\alpha_s\left(q_\perp^2\right),z\right)\widetilde{f}_b\left(\frac{x}{z},\frac{q_\perp^2}{(1-z)^2}\right). \quad (4.2)\end{aligned}$$

The KMRW angular ordered evolution equation has the following form

$$\begin{aligned}\widetilde{f}_a(x,\mu^2) &= \widetilde{f}_a(x,\mu_0^2)\Delta_a(\mu^2,\mu_0^2) \\ &+ \int_{q_0^2}^{\mu^2\left(\frac{1-x}{x}\right)^2} \frac{dq_\perp^2}{q_\perp^2}\left(\Delta_a(\mu^2,q_\perp^2)\sum_b \int_x^{1-\frac{q_\perp}{q_\perp+\mu}} dz P_{ab}^R\left(\alpha_s\left(q_\perp^2\right),z\right)\widetilde{f}_b\left(\frac{x}{z},q_\perp^2\right)\right) \quad (4.3)\end{aligned}$$

where the TMDs are defined as $\widetilde{f}(x,\mu^2,q_\perp^2) = \Delta_a(\mu^2,q_\perp^2)\sum_b \int_x^{1-\frac{q_\perp}{q_\perp+\mu}} dz P_{ab}^R\left(\alpha_s(q_\perp^2),z\right)\widetilde{f}_b\left(\frac{x}{z},q_\perp^2\right)$. KMRW is *one-step* evolution: the second scale enters only in the last step of the evolution whereas in the PB method both $k_\perp$ and μ' are calculated at each branching. Still, it is interesting to compare eq. (4.2) and eq. (4.3). Both formalisms use $q_\perp$ as the scale in α_s. Differences manifest themselves in the integration limits and in different scales in parton densities $\widetilde{f}_b$ and Sudakov form factors Δ_a. The TMD sets obtained according to KMRW angular ordering prescription, included in TMDlib and TMDplotter [13] under the name MRW-CT10nlo [14] and PB TMDs [7] are compared in the left and middle panels of fig. 4. Despite many differences, PB and KMRW are similar in the middle $k_\perp$ range compared to the scale μ . The difference in the low $k_\perp$ region comes from the intrinsic $k_\perp$ parametrization, which for KMRW is a constant parametrization and for the PB is a Gaussian smeared during the evolution process. PB and KMRW differ also in the large $k_\perp$ region: a very large $k_\perp$ tail in KMRW comes from their treatment of the Sudakov form factor for $k_\perp > \mu$. In the right of fig. 4 predictions for Z boson $p_\perp$ spectrum obtained with PB and KMRW TMDs are compared to the ATLAS data. KMRW overestimates the data in the large $p_\perp$ region.

Collins-Soper-Sterman In the following the comparison of the Sudakov form factors in the PB method and CSS formalism for the Drell-Yan (DY) cross section [4] is discussed. The PB Sudakov can be rewritten in terms of virtual pieces of the splitting functions and with angular ordering condition in the form $\Delta_a(\mu^2,\mu_0^2) = \exp\left(-\int_{\mu_0^2}^{\mu^2}\frac{dq_\perp^2}{q_\perp^2}\alpha_s(q_\perp)\left(\int_0^{1-\frac{q_\perp}{\mu}} dz\left(k_a\frac{1}{1-z}\right)-d_a\right)\right)$. The coefficients

[5] Marchesini and Webber studied the coherent branching with LO splitting functions and α_s, we use them at NLO.

[6] The difference between μ_0 and q_0 is neglected.

[7] PB TMDs were obtained with $q_0 = 1$GeV and cut in α_s forbidding the renormalization scale to go below the initial evolution scale. The starting distribution is ct10nlo.

k_q and d_q [5] in the PB Sudakov and A_1 (giving leading logarithmic (LL) contributions), B_1 and A_2 (giving together with C_1 next-to-leading logarithmic (NLL) contributions) coefficients of the CSS method are exactly the same. Because of the renormalization group equation and resummation scheme dependence the Sudakov form factor is process dependent [15]. We find a difference between B_2 CSS coefficient (giving together with A_3 and C_2 next-to-next-to leading (NNLL) logarithmic contribution) and the $2d_q^1$ coefficient in PB Sudakov being $\pi\beta_0 16\left(\frac{\pi^2}{6}-1\right)$ where β_0 is the first coefficient of the expansion of the QCD β function.

5. Conclusions

PB method allows to obtain collinear and TMD PDFs in a wide kinematic range by calculating the kinematics at each branching and to study different ordering definitions. It was shown that angular ordering condition leads to stable, z_M-independent TMDs and good description of Z boson $p_\perp$ spectrum. In this paper the PB implementation of the angular ordering condition was compared to other approaches. The PB method agrees with Marchesini's and Webber's prescription. We discussed the differences and similarities of PB and KMRW approach. We illustrated that PB includes the same LL and NLL coefficients in the Sudakov form factor as CSS formalism. The differences between NNLL coefficients in the Sudakov form factors of these two methods come from the resummation scheme dependence.

Acknowledgements The results presented in this article were obtained in collaboration with Francesco Hautmann, Hannes Jung, Aron Mees van Kampen and Lissa Keersmaekers.

References

[1] J. C. Collins, D. E. Soper and G. F. Sterman, Adv.Ser. Direct. High Energy Phys. **5** (1989) 1

[2] R. Angeles-Martinez *et al.*, Acta Phys. Polon. B **46** (2015) no.12, 2501

[3] S. Catani, M. Ciafaloni and F. Hautmann, Phys. Lett. B **242** (1990) 97
S. Catani, M. Ciafaloni and F. Hautmann, Nucl. Phys. B **366** (1991) 135

[4] J. C. Collins, D. E. Soper and G. F. Sterman, Nucl. Phys. B **250** (1985) 199

[5] F. Hautmann, H. Jung, A. Lelek, V. Radescu and R. Zlebcik, Phys. Lett. B **772** (2017) 446
F. Hautmann, H. Jung, A. Lelek, V. Radescu and R. Zlebcik, JHEP **1801** (2018) 070

[6] A. Bermudez Martinez, P. Connor, H. Jung, A. Lelek, R. Zlebcik, F. Hautmann and V. Radescu, Phys. Rev. D **99** (2019) no.7, 074008

[7] A. Lelek, doi:10.3204/PUBDB-2018-02949

[8] S. Alekhin *et al.*, Eur. Phys. J. C **75** (2015) no.7, 304

[9] G. Marchesini and B. R. Webber, Nucl. Phys. B **310** (1988) 461

[10] M. A. Kimber, A. D. Martin and M. G. Ryskin, Eur. Phys. J. C **12** (2000) 655
A. D. Martin, M. G. Ryskin and G. Watt, Eur. Phys. J. C **66** (2010) 163

[11] V. N. Gribov and L. N. Lipatov, Sov. J. Nucl. Phys. **15** (1972) 438
L. N. Lipatov, Sov. J. Nucl. Phys. **20** (1975) 94
G. Altarelli and G. Parisi, Nucl. Phys. B **126** (1977) 298
Y. L. Dokshitzer, Sov. Phys. JETP **46** (1977) 641

[12] G. Aad *et al.* [ATLAS Collaboration], Eur. Phys. J. C **76** (2016) no.5, 291

[13] F. Hautmann, H. Jung, M. Kramer, P. J. Mulders, E. R. Nocera, T. C. Rogers and A. Signori, Eur. Phys. J. C **74** (2014) 3220

[14] M. Bury, A. van Hameren, H. Jung, K. Kutak, S. Sapeta and M. Serino, Eur. Phys. J. C **78** (2018) no.2, 137

[15] S. Catani, D. de Florian and M. Grazzini, Nucl. Phys. B **596** (2001) 299

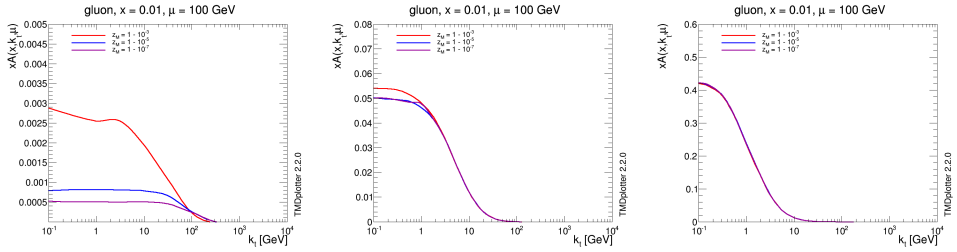

Figure 1: TMDs with $p_\perp-$ (left), virtuality (middle) and angular ordering (right) to calculate $q_\perp$, with $\alpha_s(\mu'^2)$ and for different values of z_M.

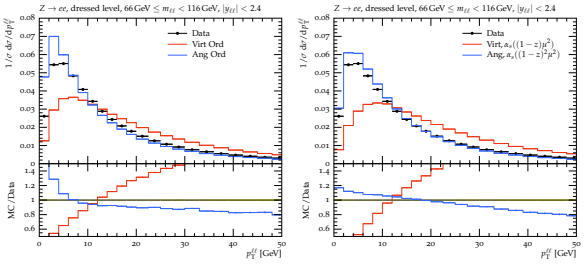

Figure 2: Predictions for the Z boson $p_\perp$ spectrum obtained with the PB TMDs with virtuality and angular ordering relation between $q_\perp$ and μ' compared to the ATLAS data. Left: with $\alpha_s(\mu'^2)$. Right: with $\alpha_s(q_\perp^2)$.

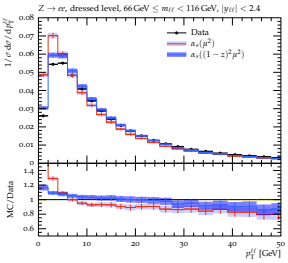

Figure 3: Predictions for the Z boson $p_\perp$ spectrum obtained with the PB TMDs from the fit for $q_\perp^2 = (1-z)^2\mu'^2$, with $\alpha_s(\mu'^2)$ and $\alpha_s(q_\perp^2)$ compared to ATLAS data.

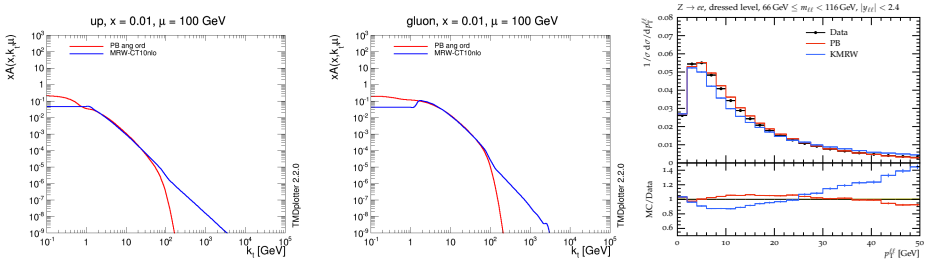

Figure 4: Comparison of KMRW and PB TMDs (left and middle). Prediction for Z boson $p_\perp$ spectrum obtained with PB TMDs and KMRW compared to 8 TeV ATLAS measurement (right).